

DESIGN AND CALCULATION OF CYLINDRICAL ELECTROSTATIC DEFLECTOR FOR THE TRANSPORT CHANNEL OF THE HEAVY ION BEAM

N. Kazarinov[†], I.Kalagin, S.Zemlyanoy

JINR, Dubna, Moscow region, 141980, Russia

[†] nyk@jinr.ru

WEPSB044

Abstract

The cylindrical electrostatic deflector is used in the beam transport channel of GALS spectrometer that is created at U400M cyclotron in Flerov Laboratory of Nuclear Reaction of Joint Institute for Nuclear research. The design and calculation of the deflector are presented in this report. The angular length of the electrodes and gap between potential electrode and screen are found by using of the minimization procedure.

INTRODUCTION

GALS is the experimental setup for selective laser ionization with gas cell [1] that will be created at U400M cyclotron in FLNR JINR [2]. The cylindrical electrostatic deflector is the optical element of the part of the channel intended for transportation of the secondary ion beam. The deflector rotates the researched ion beam from the focal plane of the spectrometric magnet onto the particle detector.

The design of the deflector is proposed in this report. In accordance with results of works [3,4] the deviation of the trajectory of the beam center of mass from the designed orbit have been minimized by appropriate choice of angular length of the deflector electrodes. The influence of the nonlinearities of the transverse electric field on the dynamics of the particles have been reduced by means of variation of angular distance between electrodes and grounded screen.

The beam dynamics simulations were performed by using the MCIB04 program code [5]. 2D field map of the deflector electric field calculated with the help of POISSON program code[6] was used in the simulations.

2D MODEL OF THE DEFLECTOR

The scheme of the deflector is shown in Fig.1.

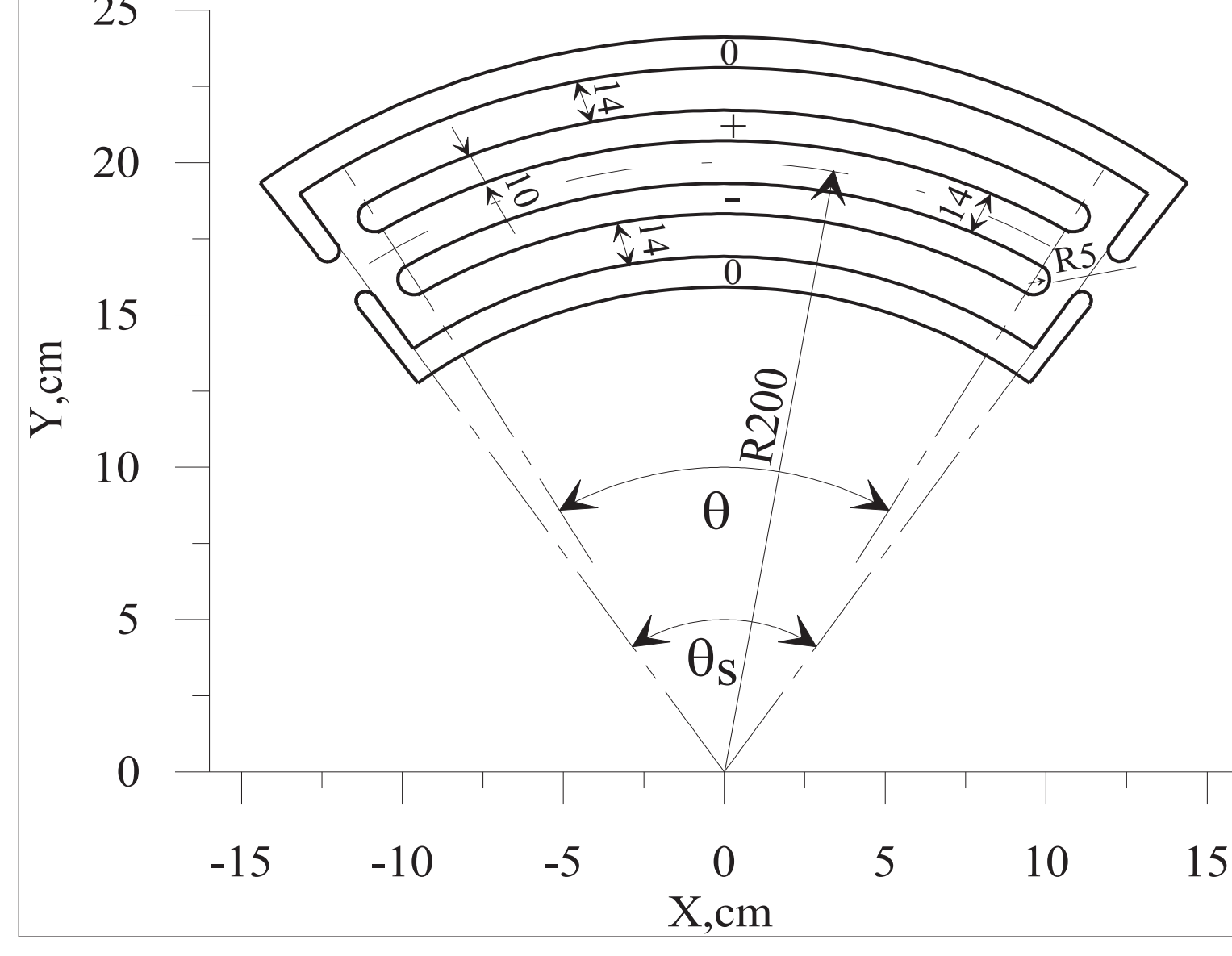


Figure 1: E(z) for one-gap buncher

The deflector consists of two electrodes under potentials U_1 (-), U_2 (+) and two grounded screens (0). The design bending radius $R = 20$ cm, design bending angle $\phi = 67$ degrees and the gap between the electrodes $d = 14$ mm. The optimal value of the angular size of the electrodes θ is equal to 62.6 degrees. The optimal angular distance between the inner end face of the screens is equal to $\theta_s = \theta + 80$. The vertical size of the electrodes (in the Z axis direction) is 80 mm.

2D computational models of the GALS deflector are shown in Fig.2. The first one (Fig.2a) corresponding to cylindrical system of coordinates ($r, z \geq 0$) has been used for evaluation of the electric field inhomogeneity inside the deflector aperture. The second one (Fig.2b) corresponding to Cartesian frame ($X \geq 0, Y \geq 0$) was used during determination of the optimum angular dimensions of the electrodes.

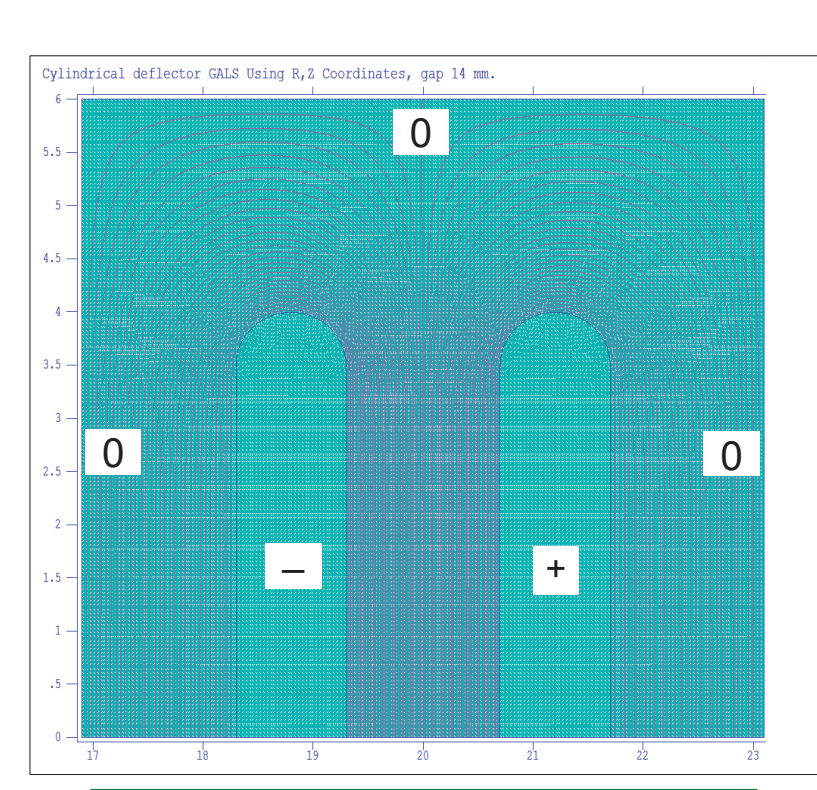


Figure 2a: 2D model in cylindrical frame

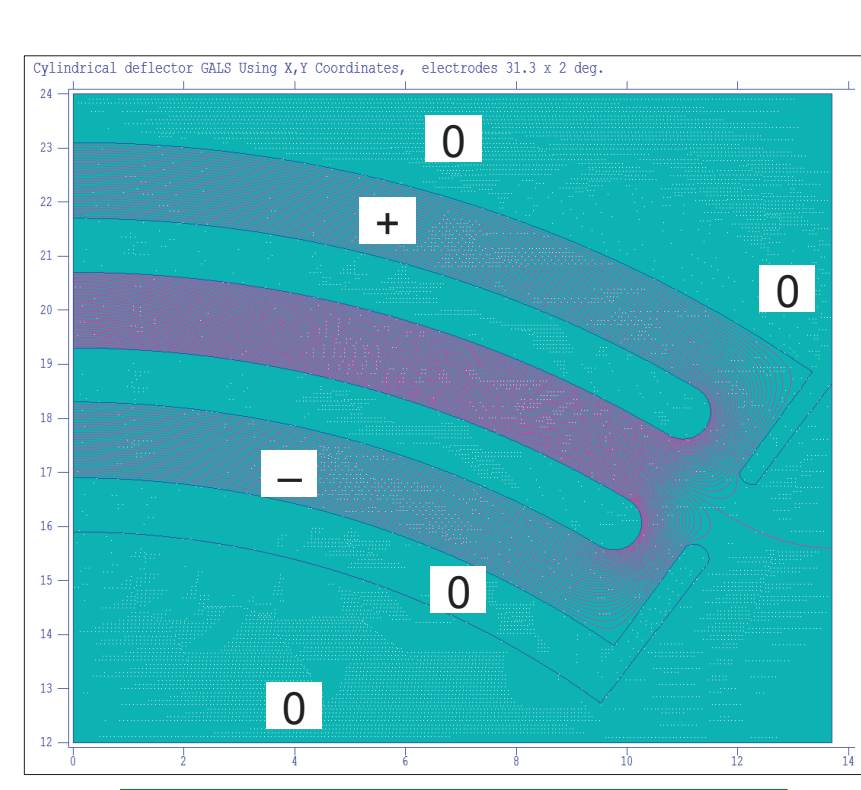


Figure 2b: 2D model in Cartesian frame

Two independent distributions of the electric field of the deflector were found for each electrode.

The electric field strength of the deflector for arbitrary voltages at the electrodes was calculated as a superposition of these distributions. The inhomogeneity of the bending electric field within the working aperture of the deflector is shown in Fig.3,4.

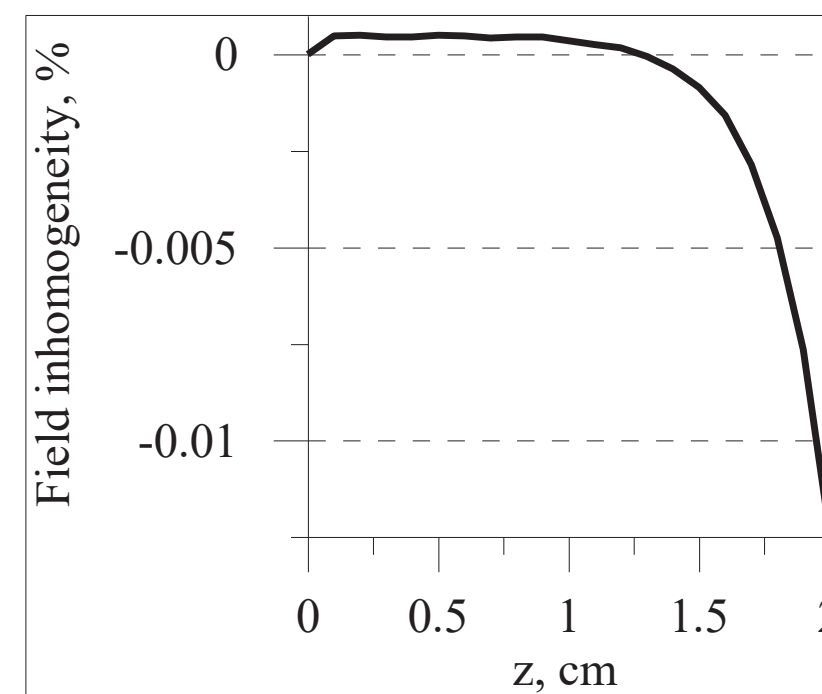


Figure 3: Inhomogeneity of bending electric field in Z-direction

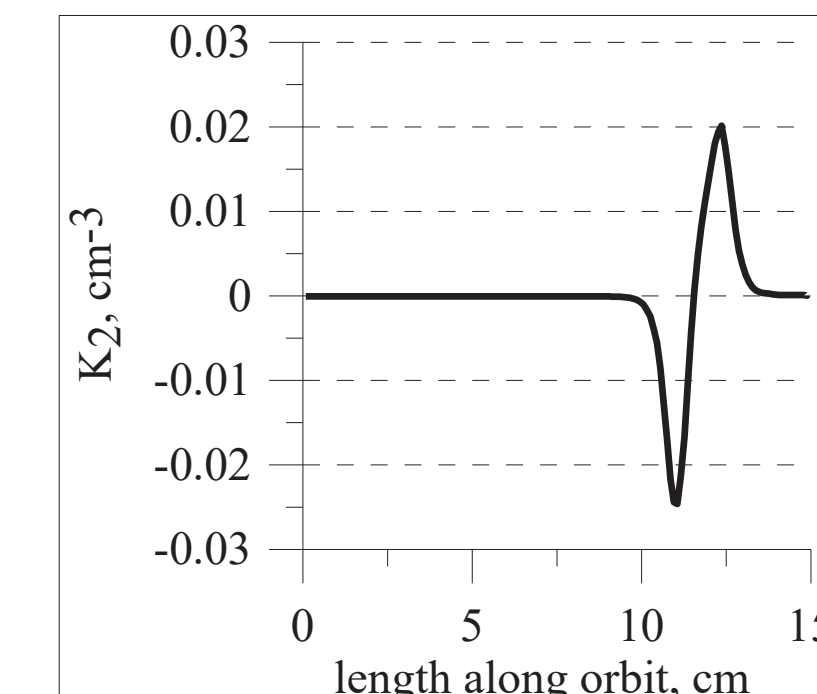


Figure 4: Sextupole coefficient K2 of bending electric field

The inhomogeneity in Z-direction is less than 0.0125% at the edge of the working area $z = \pm 2$ cm.

The dependence of the sextupole coefficient K_2 on length along orbit is shown in Fig.4. The chosen angular distance between potential electrodes and grounded screen $\Delta\theta = 8$ degrees gives the possibility to minimize the average value of sextupole coefficient at level $K_2 = 8.0 \times 10^{-5}$. It is more than three hundred times less than maximum of the absolute value of K_2 .

CALCULATED EQUILIBRIUM ORBIT

In the calculations using MCIB04 program [5] the half orbit ($X_0(s)$, $Y_0(s)$), corresponding area $X_0 \geq 0$, was considered. The initial conditions in this case were defined as follows:

$$X_0(0) = 0; X'_0(0) = 1; Y_0(0) = R_i; Y'_0(0) = 0$$

Calculated equilibrium orbit was found by means of varying the values of the voltages at the electrodes $U_{1,2}$ and the initial radius R_i of the orbit. The matching condition is the coincidence of the calculated and the design orbits and its angles at the edge of the electric field map L_E :

$$X_0(L_E) \sin(\phi/2) + Y_0(L_E) \cos(\phi/2) = R \\ X'_0(L_E) \sin(\phi/2) + Y'_0(L_E) \cos(\phi/2) = 0$$

Due to existence of three variable parameters, we can add the condition of minimum of the rms deviation between the calculated and the design orbits δ :

$$\delta = \left[\frac{1}{L_E} \int_0^{L_E} \Delta^2(s) ds \right]^{1/2} = \min \\ \Delta(s) = \begin{cases} R - \sqrt{X_0^2(s) + Y_0^2(s)} & , \phi_p \leq \frac{\phi}{2} \\ R - X_0(s) \sin\left(\frac{\phi}{2}\right) - Y_0(s) \cos\left(\frac{\phi}{2}\right), & \phi_p > \frac{\phi}{2} \end{cases}$$

Here ϕ_p is the current value of the angle of the reference particle.

In the non-relativistic approximation value of R_i is independent on the reference ion parameters (charge to mass ratio Z/A and accelerating voltage U_p). Thereby the orbit depends on only the electrodes geometry. The voltages at the electrodes $U_{1,2}$ in this case are proportional to U_p .

ELECTRODE ANGULAR SIZE

The minimum of the rms deviation δ is strongly depended on the angular size of the potential electrodes θ . The angle θ was varied in the range of 59.0-62.6 degrees to determine its optimal value. The dependences of the ratio of the bending electric field $E_n(s)$ to its value at the deflector center $E_n(0)$ for the three values of angle θ are shown in Fig.5. The angular distance $\Delta\theta$ between electrodes and screen was not changed.

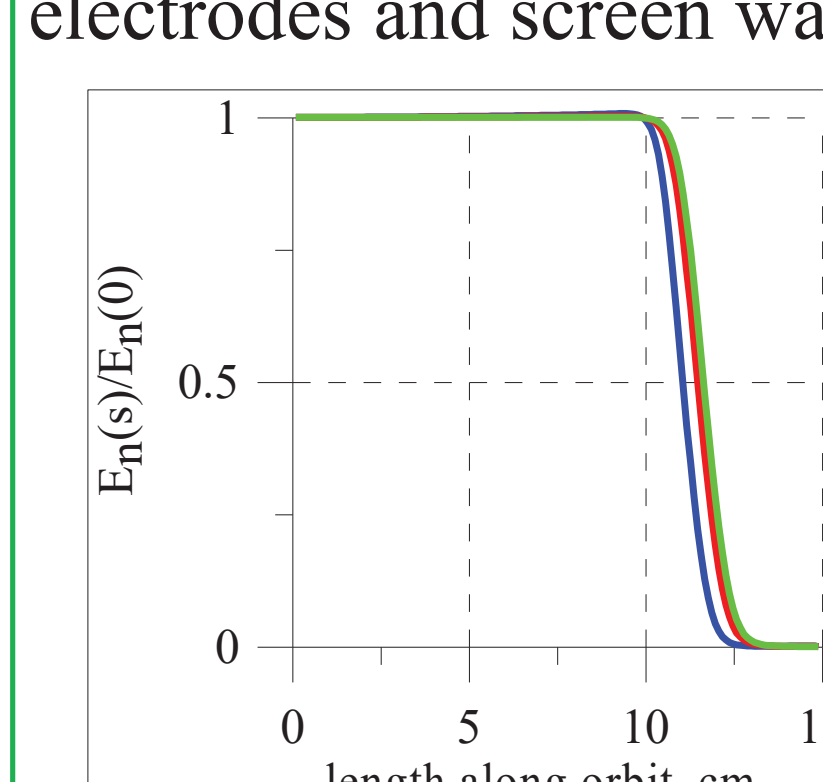


Figure 5: Bending electric field. $\theta = 59.0^\circ$ – blue line; $\theta = 61.6^\circ$ – red line; $\theta = 62.6^\circ$ – green line

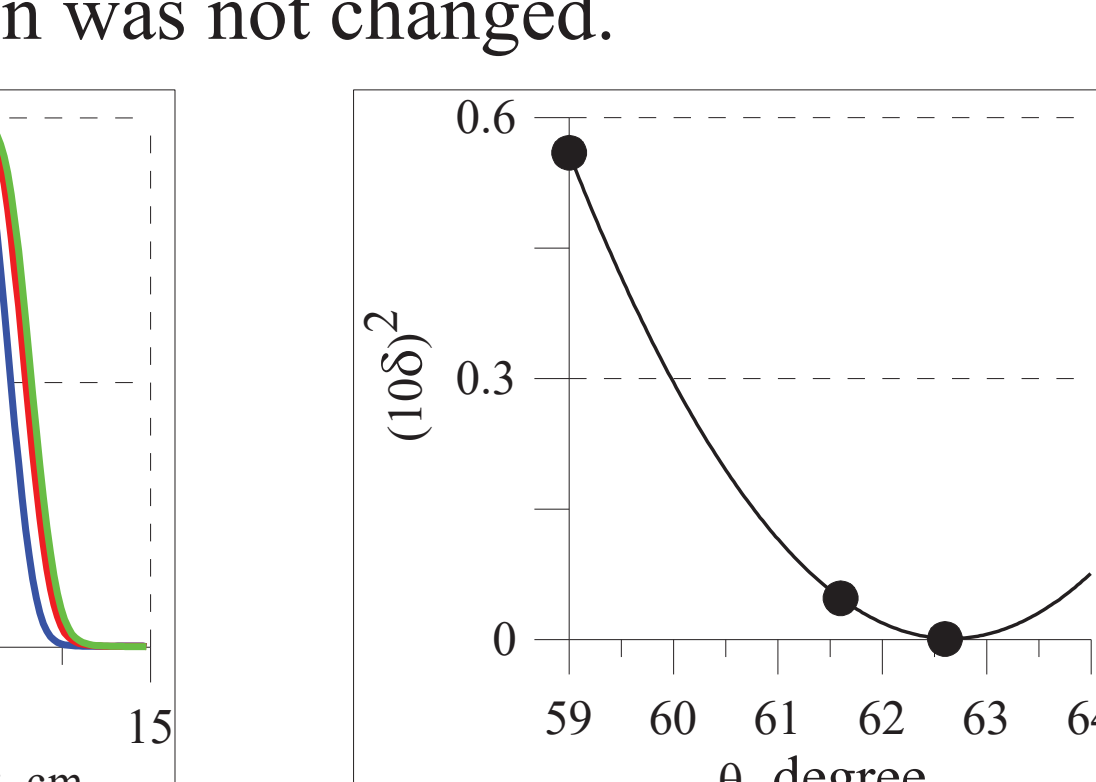


Figure 6: RMS deviation between design and calculated orbits.

The dependence of the rms deviation δ on angle θ is shown in Fig.6. The dots mark the calculation results for the three field maps. The global minimum is corresponded to angle $\theta = 62.60^\circ$.

DEFLECTOR BASIC PARAMETERS

The calculated orbit and deviation $\Delta(s)$ for the optimum value of the angle $\theta = 62.60$ are shown in Fig.7. As may be seen from Fig.7b the maximal deviation does not greater than 0.12 mm. The maximum accelerator voltage of GALS setup $U_p = 40$ kV and corresponding voltages at the electrodes are $U_1 = -2.866$ kV and $U_2 = 2.754$ kV.

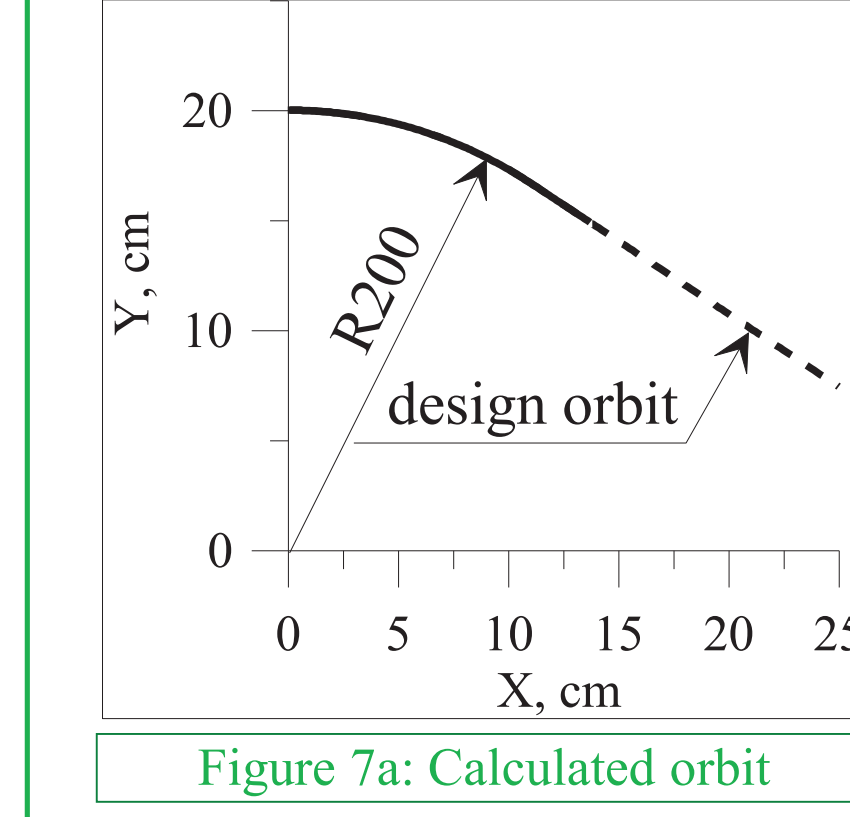


Figure 7a: Calculated orbit

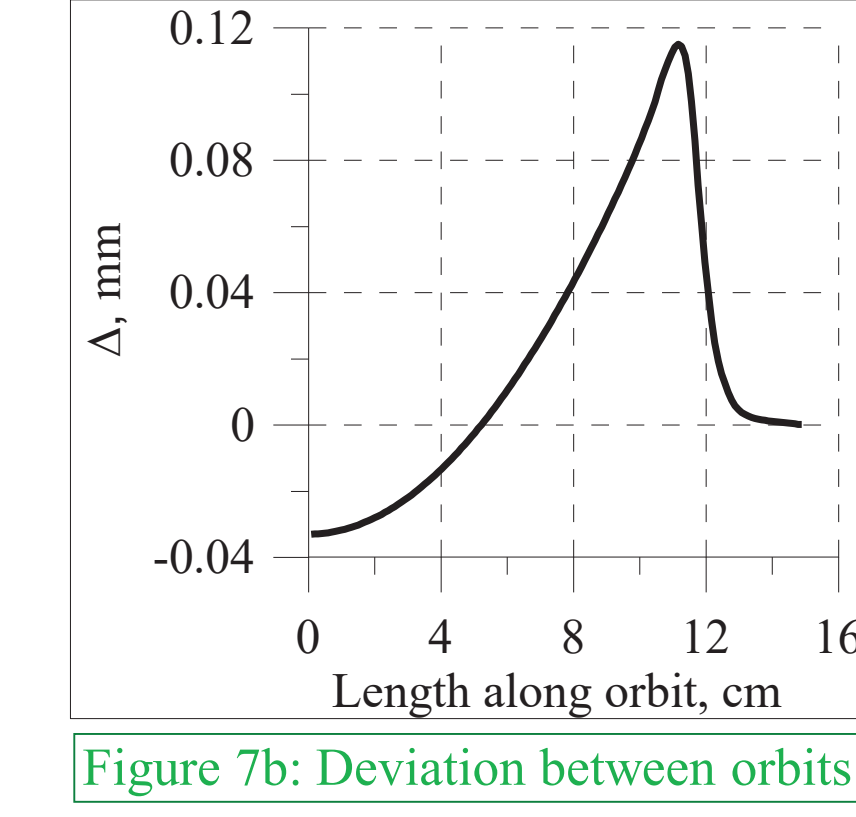


Figure 7b: Deviation between orbits

The distributions of bending $E_n(s)$ and tangent $E_t(s)$ electric fields at calculated orbit are shown in Fig.8.

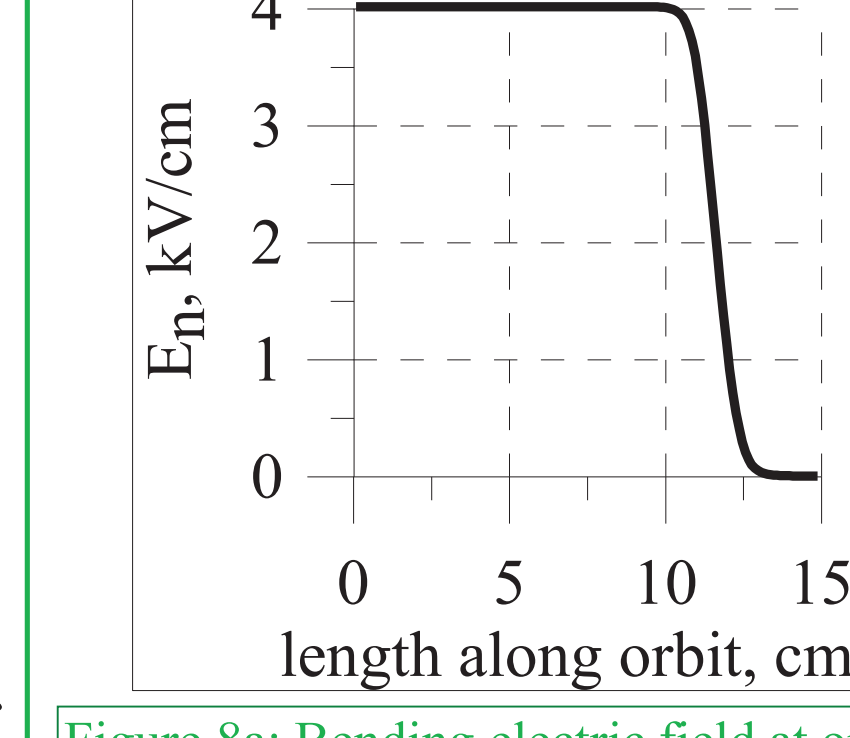


Figure 8a: Bending electric field at orbit

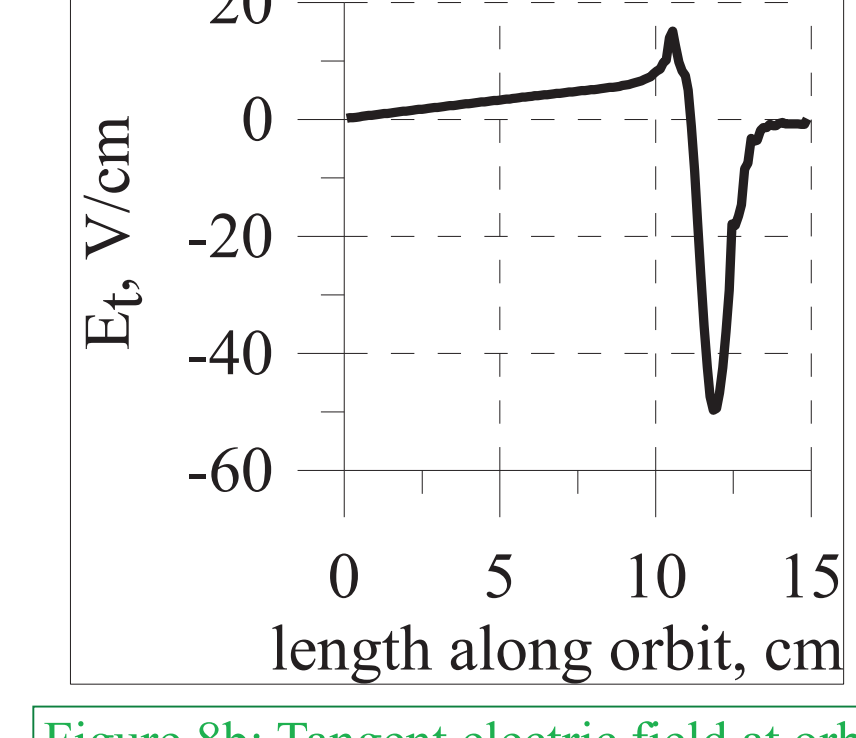


Figure 8b: Tangent electric field at orbit

The effective radius R_{eff} of the deflector defines the horizontal focusing of the beam and may be used in calculation of the beam transport line. It may be evaluated by using the effective quadrupole coefficient $K_1(s)$ of the cylindrical electrostatic deflector [7]:

$$K_1(s) = K(s) \left(3K(s) + \frac{1}{E_n} \frac{\partial E_n}{\partial x} \right)$$

Here $K(s)$ is curvature of the orbit and differentiation is carried out in the direction perpendicular to the orbit. The dependence of coefficient $K_1(s)$ on distance along the calculated orbit is shown in Fig.9.

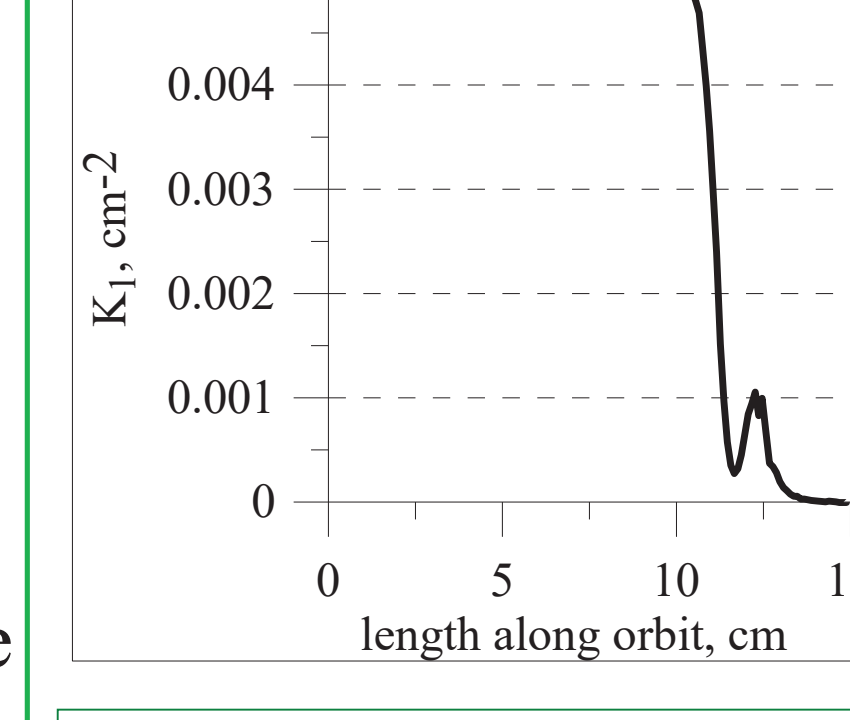


Figure 9: Quadrupole coefficient $K_1(s)$

The effective radius of the deflector may be introduced in accordance with the formula:

$$R_{eff} = \frac{\phi}{\langle K_1 \rangle L_E}$$

Here $\langle K_1 \rangle$ is average value of the quadrupole coefficient $K_1(s)$ along the orbit.

The calculation gives the value of the effective radius of the deflector $R_{eff} = 20.8$ cm for the chosen parameters of the deflector.

REFERENCES

- [1] S.Zemlyanoy, V.Zagrebaev, E.Kozulin, Yu.Kudryavtsev, V.Fedorosev, R.Bark and Z.Janas, "GALS – setup for production and study of multi-nucleon transfer reaction products: present status", Journal of Physics: C. S. 724 (2016) 012057
- [2] B.Gikal et al., "The JINR FLNR Heavy Ion Cyclotron Complex", WEYMH03, these proceedings.
- [3] H. Hubner and H. Wolnik, "The Design of Magnetic Field Elements," Nucl. Instrum. Methods 86, 141 (1970).
- [4] I.A.Ivanenko, N.Yu.Kazarinov, "Optimization of the Magnetic Field in the Analyzing Magnet of the Axial Injection Beam Line of the Cyclotron DC-280, "Physics of Particles and Nuclei Letters, 2014, Vol. 11, No. 6, pp. 756–762, ISSN 1547-4771.
- [5] V.Alexandrov, N.Kazarinov, and V.Shevtssov, "Multi-Component Ion Beam code – MCIB04," Proc. of XIX-th Russian Part. Accel. Conf. RUPAC2004. Dubna, Russia. 4-9 October 2004.
- [6] Reference Manual for the POISSON/SUPERFISH Group of Codes, Los Alamos National Laboratory Report LA-UR-87-126 (1987)
- [7] N.Kazarinov, I.Ivanenko, "Electrostatic Deflector of the Cyclotron DC-280 Axial Injection Channel", Proceedings of the 13th International Conference on Heavy Ion Accelerator Technology, HIAT2015, September 7-11, Yokohama, Japan, p.71.